Two-Magnon Resonant Raman Scattering in MnF_2

Nabil M. Amer
Department of Physics, University of California, Berkeley, California 94720

and

Tai-chang Chiang and Y. R. Shen
Department of Physics, University of California, Berkeley, California 94720, and
Inorganic Materials Research Division, Lawrence Berkeley Laboratory, Berkeley, California 94720

(Received 24 March 1975)

Resonant Raman scattering in MnF_2 around the magnon sidebands selects a particular set of two-magnon modes to be resonantly enhanced. Consequently, the two-magnon line shifts with the laser frequency and two two-magnon lines can show up simultaneously. A simple theory is used to interpret the experimental results.

Resonant Raman scattering (RRS) in solids has recently received much attention.[1] We report here the first investigation on RRS in a magnetically ordered crystal, e.g., MnF_2 in the antiferromagnetic phase. Because of space limitation, we shall discuss only RRS by two magnons in MnF_2 in some detail.

The magnon spectrum of the antiferromagnetic MnF_2 is well known.[2] The optical properties of MnF_2 have also been well studied, especially those involving magnons.[3-5] There is a set of sharp absorption lines around 18 450 cm^{-1} (see Fig. 1) arising from transitions within the ${}^6A_{1g}({}^6S) \rightarrow {}^4T_{1g}({}^4G)$ manifold.[3] Lines e_1 and e_2 are due to creation of E_1 and E_2 excitons, respectively, via direct magnetic-dipole transitions while lines σ_1, π_1, and σ_2 are the corresponding magnon sidebands. In the luminescence spectrum,[5] direct and magnon-assisted recombinations of the E_1 excitons give rise to the e_{1L} and σ_{1L} (π_{1L}) luminescence lines, respectively.

The Raman spectrum of MnF_2 has also been thoroughly studied.[6-8] It consists of four phonon modes and one two-magnon line. No one-magnon line has yet been observed. We are interested in the changes of the Raman and luminescence spectra when the excitation scans through the absorption lines in Fig. 1.

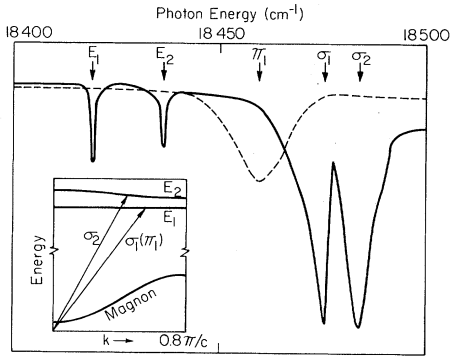

FIG. 1. Absorption spectrum of MnF_2 at 1.6 K between 18 400 and 18 500 cm^{-1}. The solid and the dashed curves are for polarizations perpendicular and parallel to the $\hat{c}$ axis, respectively. The inset is a sketch of the relevant energy levels.

Theoretically, the peak position and the cross section of the two-magnon line for excitation near σ_1, π_1, and σ_2 lines can be obtained following, for example, Loudon's derivation.[4,6,7] The spin Hamiltonian is of the form (unless specified, we use the notations of Ref. 6)

$$H_s = \sum_{\langle i,j\rangle} \sum_{\alpha,\beta} C_{ij}{}^{\alpha\beta} E_l{}^{\alpha} E_s{}^{\beta *} S_i^- S_j^+ , \tag{1}$$

where

$$C_{ij}{}^{\alpha\beta} = A_{ij}{}^{\alpha\beta} + B_{ij}{}^{\alpha\beta},$$

$$A_{ij}{}^{\alpha\beta} = \sum_{\mu,\nu} \frac{\langle g_i{\downarrow} g_j{\uparrow} | e r_\beta | g_i{\downarrow} \nu_j{\uparrow}\rangle \langle g_i{\downarrow} \nu_j{\uparrow} | V_{ex} | \mu_i{\uparrow} g_j{\downarrow}\rangle \langle \mu_i{\uparrow} g_j{\downarrow} | e r_\alpha | g_i{\uparrow} g_j{\downarrow}\rangle}{(E_\nu - \hbar\omega_s)(E_\mu - \hbar\omega_l)} + 11 \text{ similar terms},$$

$$B_{ij}{}^{\alpha\beta} \cong \sum_{\mu,\nu} \frac{\langle g_i{\downarrow} g_j{\uparrow} | e r_\beta | \nu_i{\downarrow} g_j{\uparrow}\rangle \langle \nu_i{\downarrow} g_j{\uparrow} | V | e_i{\downarrow} g_j{\uparrow}\rangle \langle e_i{\downarrow} g_j{\uparrow} | V_{ex} | \mu_i{\uparrow} g_j{\downarrow}\rangle \langle \mu_i{\uparrow} g_j{\downarrow} | e r_\alpha | g_i{\uparrow} g_j{\downarrow}\rangle}{(E_\nu - \hbar\omega_s)(E_\mu - \hbar\omega_l)\hbar(\omega_l - \omega_E - \omega_m + i\Gamma)} .$$

In the above equations, $\langle g_i|$ is the ground state of the ith Mn ion, $\langle\mu|$ and $\langle\nu|$ are the allowed excited states with energies E_μ and E_ν, respectively, and $\langle e|$ is either the E_1 or the E_2 excitonic state with its energy denoted by $\hbar\omega_E$. The magnon frequency is ω_m. The quantities $E_l{}^\alpha$ and $E_s{}^\beta$ represent the α component of the exciting field and the β component of the scattered field, respectively, and V and V_{ex} are, respectively, the direct and exchange terms of the Coulomb interaction. From Eq. (1) we find for the two-magnon Raman cross section

$$\frac{d\sigma_{\alpha\beta}}{d\omega_s}=\sum_{\vec{k}}\left|a_{\alpha\beta}+\frac{b_{\alpha\beta}}{\omega_l-\omega_E(\vec{k})-\omega_m(\vec{k})+i\Gamma}\right|^2 f_{\alpha\beta}(\vec{k})\,\frac{\Gamma'}{|\omega_l-\omega_s-2\omega_m(\vec{k})+i\Gamma'|^2}\,, \tag{2}$$

where $a_{\alpha\beta}$ and $b_{\alpha\beta}$ are constant coefficients if we assume the matrix elements in Eq. (1) are constant and $f_{\alpha\beta}(\vec{k})$ is a function of $\vec{k}$. Since the $b_{\alpha\beta}$ term is obtained from higher-order perturbation than the $\alpha_{\alpha\beta}$ term, the former should be negligible in comparison with the latter unless the excitation frequency is close to one of the magnon sidebands, i.e., $\omega_l\sim\omega_E+\omega_m(\vec{k})$. Near such a resonance, if we use the approximation $|x+i\Gamma|^{-2}\approx\pi\delta(x)/\Gamma$, we can write

$$d\sigma_{\alpha\beta}/d\omega_s\cong(d\sigma_{\alpha\beta}/d\omega_s)_{NR}+(d\sigma_{\alpha\beta}/d\omega_s)_R\,, \tag{3}$$

with

$$(d\sigma_{\alpha\beta}/d\omega_s)_{NR}=(\pi|a_{\alpha\beta}|^2/\Gamma')\textstyle\sum_{\vec{k}}f_{\alpha\beta}(\vec{k})\delta(\omega_l-\omega_s-2\omega_m(\vec{k}))\,, \tag{3a}$$

$$(d\sigma_{\alpha\beta}/d\omega_s)_R=(\pi^2|b_{\alpha\beta}|^2/\Gamma\Gamma')\textstyle\sum_{\vec{k}}f_{\alpha\beta}(\vec{k})\,\delta(\omega_l-\omega_E(\vec{k})-\omega_m(\vec{k}))\delta(\omega_l-\omega_s-2\omega_m(\vec{k}))\,. \tag{3b}$$

The total two-magnon Raman cross section is then given by

$$\sigma_{\alpha\beta}=(\sigma_{\alpha\beta})_{NR}+(\sigma_{\alpha\beta})_R\,, \tag{4}$$

where $(\sigma_{\alpha\beta})_R\propto[d\sigma_{\alpha\beta}(\omega_l-\omega_s=2\omega_l-2\omega_E)/d\omega_s]_{NR}$. Equation (3b) shows that at resonance, if $(d\sigma_{\alpha\beta}/d\omega_s)_R>(d\sigma_{\alpha\beta}/d\omega_s)_{NR}$, the peak position of the two-magnon line is determined by

$$\omega_l-\omega_s=2\omega_m(\vec{k})=2\omega_l-2\omega_E(\vec{k}). \tag{5}$$

The above results are easy to understand physically since the resonant part can be considered as due to a magnon-assisted absorption immediately followed by a magnon-assisted emission.

A continuous-wave dye laser with a linewidth of 0.2 cm^{-1} was used as the excitation source and the sample was immersed in superfluid He at 1.6°K. The luminescence spectrum was essentially identical to those reported in the literature but with fewer impurity lines, none in the range between 18 340 and 18 440 cm^{-1}, except the one (denoted by I in Fig. 2) overlapping with the σ_{1L} line.[5]

Our results on resonance fluorescence and RRS by phonons in MnF_2 will be reported elsewhere. Here, we discuss only RRS by two magnons. We found that the two-magnon line showed a resonance enhancement at the magnon sidebands but not at the e_1 and e_2 exciton lines, just as we expected. Figure 2 shows a set of two-magnon Raman spectra at several different excitation frequencies around σ_1 and σ_2. It is seen that the two-magnon line (denoted by M) varies in frequency with ω_l. Deep in resonance, the line is considerably sharper (limited by instrument resolution in Fig. 2). When ω_l falls in the region where σ_1 and σ_2 overlap, two two-magnon lines show up, due to simultaneous resonances in σ_1 and σ_2 with two different sets of magnon modes involved. We have plotted the Raman peak shift of the two-magnon line as a function of ω_l in Fig. 3(a), and the corresponding Raman cross section σ_{xy} (corrected for absorption) versus ω_l in Fig. 3(b). The

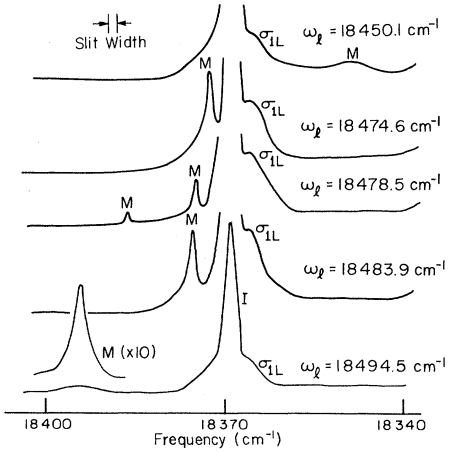

FIG. 2. Two-magnon Raman spectra (denoted by M) at several different excitation frequencies ω_l. Peaks I and σ_{1L} correspond to impurity and magnon-assisted luminescence lines, respectively.

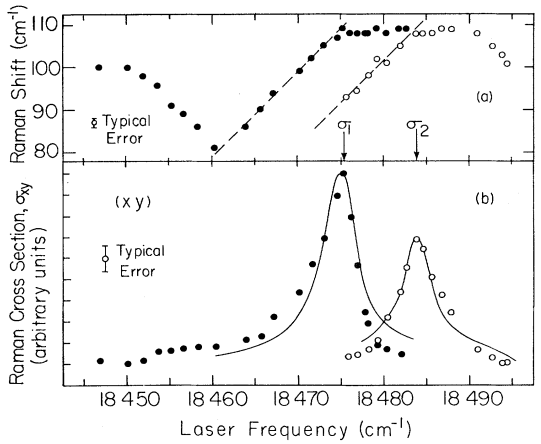

FIG. 3. (a) Two-magnon Raman shift and (b) two-magnon Raman cross section as functions of the excitation frequency ω_l. The exciting and the scattering radiations are polarized along $\hat{y}$ and $\hat{x}$, respectively ($\hat{x}, \hat{y} \perp \hat{c}$).

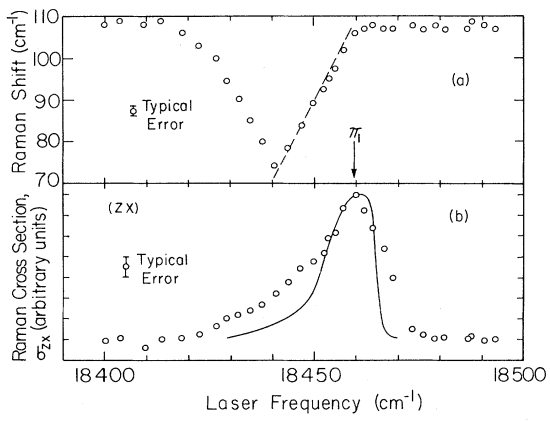

FIG. 4. (a) Two-magnon Raman shift and (b) two-magnon Raman cross section as functions of the excitation frequency ω_l. The exciting and the scattering radiations are polarized along $\hat{z}$ and $\hat{x}$, respectively ($\hat{x} \perp \hat{c}$ and $\hat{z} \parallel \hat{c}$).

same results for σ_{xz} are given in Fig. 4.

The results of Figs. 3 and 4 agree well with our earlier description. When $(d\sigma_{\alpha\beta}/d\omega_s)_R > (d\sigma_{\alpha\beta}/d\omega_s)_{NR}$, the Raman shift should obey Eq. (5). We find that we can indeed fit that portion of the data by Eq. (5) assuming $\omega_E(\vec{k})$ is independent of $\vec{k}$. This is shown by the straight lines in Figs. 3(a) and 4(a). The values of constant ω_E deduced from the fit, for RRS near σ_1, σ_2, and π_1 peaks, respectively, are $\omega_E(\sigma_1) = 18\,420.7$ cm^{-1}, $\omega_E(\sigma_2) = 18\,429.5$ cm^{-1}, and $\omega_E(\pi_1) = 18\,405$ cm^{-1}. If σ_1 (π_1) and σ_2 are indeed magnon sidebands of e_1 and e_2 and if the assumption of dispersionless $\omega_E(\vec{k})$ is correct, then $\omega_E(\sigma_1)$ and $\omega_E(\pi_1)$ should be equal to the frequency of the e_1 absorption peak and $\omega_E(\sigma_2)$ to the frequency of the e_2 peak. The observed e_1 and e_2 lines are at $\omega_{e_1} = 18\,419.5$ cm^{-1} and $\omega_{e_2} = 18\,436.5$ cm^{-1}. The agreement between $\omega_E(\sigma_1)$ and ω_{e_1} is within the experimental uncertainty, supporting the previous suggestion that the dispersion of the E_1 exciton is less than 0.5 cm^{-1}.[5] There is a discrepancy of 7 cm^{-1} between $\omega_E(\sigma_2)$ and ω_{e_2}. This indicates that the E_2 exciton has a negative dispersion of 7 cm^{-1} from the zone center to the zone edge, in agreement with the 6.2 cm^{-1} estimate of Sell, Greene, and White.[3] The fact that the data can still be fitted with a straight line suggests a negligible dispersion of E_2 near the zone edge. There is a big discrepancy of 14.5 cm^{-1} between $\omega_E(\pi_1)$ and ω_{e_1}. Since we know E_1 is nearly dispersionless, this makes us suspect that π_1 is not a magnon sideband of E_1 but of a lower-energy excitonic state. However, no such state has been found in absorption. Similar difficulty exists in the interpretation of the π_1 absorption band.[3] Sell, Greene, and White[3] have found that the observed π_1 peak is shifted by about -9 cm^{-1} from the predicted position. The above discrepancies about σ_2 and π_1 could also be due to exciton-magnon interaction.[9] Both exciton-magnon and magnon-magnon interactions were neglected in deriving Eq. (5).

The rest of the data in Figs. 3(a) and 4(a) can be interpreted qualitatively as follows. On the low-energy side of a magnon sideband, when $(d\sigma_{\alpha\beta}/d\omega_s)_{NR}$ becomes more and more dominant over $(d\sigma_{\alpha\beta}/d\omega_s)_R$, the two-magnon line gradually changes into its off-resonance line shape and the Raman peak shift moves towards the off-resonance value. On the high-energy side close to the peak of a magnon sideband, the resonance enhancement of those two-magnon modes near the zone edge still dominates [consider Eq. (2) with finite damping constants], leaving the peak position of the two-magnon line more or less unchanged.

We have also found that Eq. (4) describes the observed two-magnon resonance Raman enhancement near magnon sidebands quite well. In Figs. 3(b) and 4(b), the theoretical curves are obtained from Eq. (4) using the experimental line shape of $(d\sigma_{\alpha\beta}/d\omega_s)_{NR}$ and with $(\sigma_{\alpha\beta})_R$ normalized to its peak value. The discrepancy between theory and experiment is probably a result of the δ-function

approximation in the theoretical derivation.

In summary, we have observed two-magnon RRS in MnF_2 around the magnon sidebands. The mechanism for the two-magnon RRS is different from that for the nonresonant case. With a given excitation frequency ω_l, it selects a particular set of two-magnon modes to be most strongly resonantly enhanced. Consequently, because of the presence of magnon dispersion, the two-magnon line shifts in frequency as ω_l varies, and two two-magnon lines show up when simultaneous resonance with two magnon sidebands occurs. The resonance enhancement agrees quite well with a simple theoretical description.

We are indebted to Professor Y. Petroff for his technical help. This work was supported by the U. S. Energy Research and Development Administration.

[1]See, for example, P. Y. Yu and Y. R. Shen, Phys. Rev. Lett. 32, 373, 939 (1974).

[2]R. A. Erickson, Phys. Rev. 90, 779 (1953); A. Okazaki and K. C. Turberfield, Phys. Lett. 8, 9 (1964).

[3]D. D. Sell, R. L. Greene, and R. M. White, Phys. Rev. 158, 489 (1967).

[4]R. Loudon, Advan. Phys. 17, 243 (1968).

[5]R. E. Dietz, A. E. Meixner, H. J. Guggenheim, and A. Misetich, J. Luminesc. 1,2, 279 (1970); R. E. Dietz, A. E. Meixner, H. J. Guggenheim, and A. Misetich, Phys. Rev. Lett. 21, 1067 (1968).

[6]P. A. Fleury, S. P. S. Porto, and R. Loudon, Phys. Rev. Lett. 18, 658 (1967).

[7]P. A. Fleury and R. Loudon, Phys. Rev. 166, 514 (1968).

[8]S. P. S. Porto, P. A. Fleury, and T. C. Damen, Phys. Rev. 154, 522 (1967).

[9]Y. Tanabe, K.-I. Gondaira, and H. Murata, J. Phys. Soc. Jpn. 25, 1562 (1968).

Possibly Mixed Valency of Uranium in $UNi_{5-x}Cu_x$

H. J. van Daal, K. H. J. Buschow, P. B. van Aken, and M. H. van Maaren
Philips Research Laboratories, Eindhoven, The Netherlands
(Received 26 September 1974)

This paper reports the lattice constant at room temperature and the susceptibility, specific heat, electrical resistivity, and absolute Seebeck coefficient of compounds $UNi_{5-x}Cu_x$ ($0 \leq x \leq 5$) as a function of temperature. It is suggested that the drastic change in the properties of these compounds when x, increasing from 0, comes into the range of 4 to 5 is caused by a change of the uranium ions from a U^{4+} to a mixed U^{4+}-U^{3+} state.

It is already known from susceptibility (χ) measurements,[1] in the temperature range of 4 to 900 K, and from neutron diffraction data[2] that UCu_5 is an antiferromagnet with a Néel temperature (T_N) of 15 K. It is concluded in Ref. 1 from the approximate Curie-Weiss behavior of χ at temperatures above 400 K that the effective moment (p_{eff}) per uranium equals $3.6\mu_B$, and that the uranium ions are in the U^{4+} ($5f^2$) state. A different conclusion is reached by Brodsky and Bridger,[3] where the data bear upon the susceptibility and resistivity (ρ) of UNi_5 and UCu_5 (2 to 300 K), namely that χ in UCu_5 at $T > T_N$ follows a modified Curie-Weiss law with $p_{eff} \approx 2.3\mu_B$, corresponding to the U^{2+} ($5f^4$) state. For UNi_5, a similar analysis led to $p_{eff} \approx 0.15\mu_B$. Not much different results were obtained on samples either as cast or annealed at 1210 K for 5 days. On the other hand, annealing was reported to have a large influence on ρ-T data obtained on UCu_5.

In this paper it is suggested that in UCu_5 the uranium ions are neither tetravalent nor divalent but mixed tetravalent and trivalent. Indications of a mixed-valency state are derived not only from the lattice constant a of cubic ($AuBe_5$ type) pseudobinary compounds $UNi_{5-x}Cu_x$ ($0 \leq x \leq 5$) but also from the specific heat C_p, ρ, and Seebeck coefficient S. Another indication is the hypersensitivity of ρ of UCu_5 to deviations from stoichiometry and annealing. The choice of the valency states U^{4+} and U^{3+} is based on χ data. The samples investigated, unless stated otherwise, were as cast. They were checked by x-ray analysis to be single phase.

The variation with x of the lattice constant is shown in the inset of Fig. 1. It is seen that for values of x up to 3 the increase of a proceeds linearly, while there is an additional increase of a for $x > 3$. The increase of the unit-cell volume when going from UNi_5 to UCu_5 amounts to 11.2%.